RIBEYE, a Component of Synaptic Ribbons: A Protein's Journey through Evolution Provides Insight into Synaptic Ribbon Function

Frank Schmitz,*†‡ Andreas Königstorfer,†
and Thomas C. Südhof*§
*Howard Hughes Medical Institute
Center for Basic Neuroscience
Department of Molecular Genetics
The University of Texas Southwestern
   Medical Center
Dallas, Texas 75390
†Department of Molecular Neurobiology
Max-Planck-Institut für experimentelle Medizin
37075 Göttingen
‡Leibniz-Institut für Neurobiologie
Abteilung Neurochemie/Molekularbiologie
39118 Magdeburg
Federal Republic of Germany

Summary

Photoreceptor cells utilize ribbon synapses to transmit sensory signals at high resolution. Ribbon synapses release neurotransmitters tonically, with a high release rate made possible by continuous docking of synaptic vesicles on presynaptic ribbons. We have partially purified synaptic ribbons from retina and identified a major protein component called RIBEYE. RIBEYE is composed of a unique A domain specific for ribbons, and a B domain identical with CtBP2, a transcriptional repressor that in turn is related to 2-hydroxyacid dehydrogenases. The A domain mediates assembly of RIBEYE into large structures, whereas the B domain binds NAD^+ with high affinity, similar to 2-hydroxyacid dehydrogenases. Our results define a unique component of synaptic ribbons and suggest that RIBEYE evolved in vertebrates under utilization of a preexisting protein to build a unique scaffold for a specialized synapse.

Introduction

Ribbon synapses of the vertebrate retina are unique chemical synapses characterized by presynaptic ribbons, sheet-like organelles with a lamellar organization (reviewed by Dowling, 1987; Sterling, 1998). In presynaptic nerve terminals of photoreceptors, ribbons are located perpendicular to the active zone of the plasma membrane where synaptic vesicles undergo exocytosis (Gray and Pease, 1971; Schaeffer et al., 1982). Numerous synaptic vesicles are attached to both faces of a ribbon by short filaments and reach the active zone at the bottom edge of the ribbon. Active zones of ribbon synapses, similar to those of conventional synapses, contain docked vesicles ready for exocytosis but are longer than those of conventional synapses. Classic ribbon synapses are found only in vertebrates, where they are best characterized in sensory synapses with extraordinary

signaling requirements. In retina, photoreceptor and bipolar cells contain classic ribbon synapses (Dowling, 1987; Sterling. 1998); in addition, hair cells in the cochlea and pinealocytes in the epiphysis have presynaptic dense bodies that resemble ribbons and probably function as such (Smith and Sjöstrand, 1961; Hopsu and Arstila, 1964; Jastrow et al., 1997; Lenzi et al., 1999). In invertebrates such as *Drosophila*, T-shaped presynaptic structures that are similar to ribbons and probably function analogously are found in photoreceptor nerve terminals, neuromuscular junctions, and other synapses (Trujillo-Cenoz, 1972; Wan et al., 2000). However, the invertebrate structures are probably different from vertebrate synaptic ribbons because they have a distinct shape and texture and are directly connected to the active zones, whereas synaptic ribbons are not contiguous with active zones.

Physiologically, ribbon synapses are characterized by a high rate of tonic neurotransmitter release mediated by continuous synaptic vesicle exoctyosis (Dowling, 1987; Sterling, 1998). It is generally thought that ribbon synapses are specialized for rapid supply of synaptic vesicles for release and that this is achieved by fast delivery of synaptic vesicles to the active zone on the ribbon, analogous to a conveyor belt. A typical synapse formed by a vertebrate rod photoreceptor contains a single large crescent-shaped ribbon with an active zone at the base (Rao-Mirotznik et al., 1995). The ribbon tethers $\sim$600 synaptic vesicles, whereas the active zone contains $\sim$130 docked vesicles. Exocytosis of docked vesicles in ribbon synapses is stimulated by Ca^{2+}, similar to conventional synapses but at a higher rate. Per ribbon, moderate Ca^{2+} levels induce release of $\sim$50 vesicles/s, whereas maximal Ca^{2+} concentrations cause rates as high as 500 vesicles/s (Parsons et al., 1994; Rieke and Schwartz, 1996; von Gersdorff et al., 1996). The high rate of release per ribbon is astounding, considering that a hippocampal synapse exhibits maximal release rates of only $\sim$20 vesicles/s (Stevens and Tsujimoto, 1995). This high release rate is probably made possible by the function of the ribbons in providing a reservoir of release-ready synaptic vesicles that are immediately available for fusion. At a ribbon synapse, stimulation by high Ca^{2+} triggers release of the entire pool of vesicles tethered to the ribbon on a millisecond timeframe (von Gersdorff et al., 1996), suggesting that the sizable ribbon surface allows priming of a large number of vesicles that are then immediately available for exocytosis. Dependent on Ca^{2+}, primed vesicles then rapidly move down the ribbons to the active zone for fusion. As a result, the rate of release at ribbon synapses can be fine-tuned over a wide range, indicating that ribbon synapses evolved to allow fast graded transmission at specialized sensory synapses (Juusola et al., 1996). The sensory systems involved, vision and hearing, require the highest rate of information transfer and the finest sensory discrimination, highlighting the importance of ribbon synapses for the normal function of the vertebrate brain.

Detailed studies of the distribution of various presynaptic proteins in ribbon synapses demonstrated that

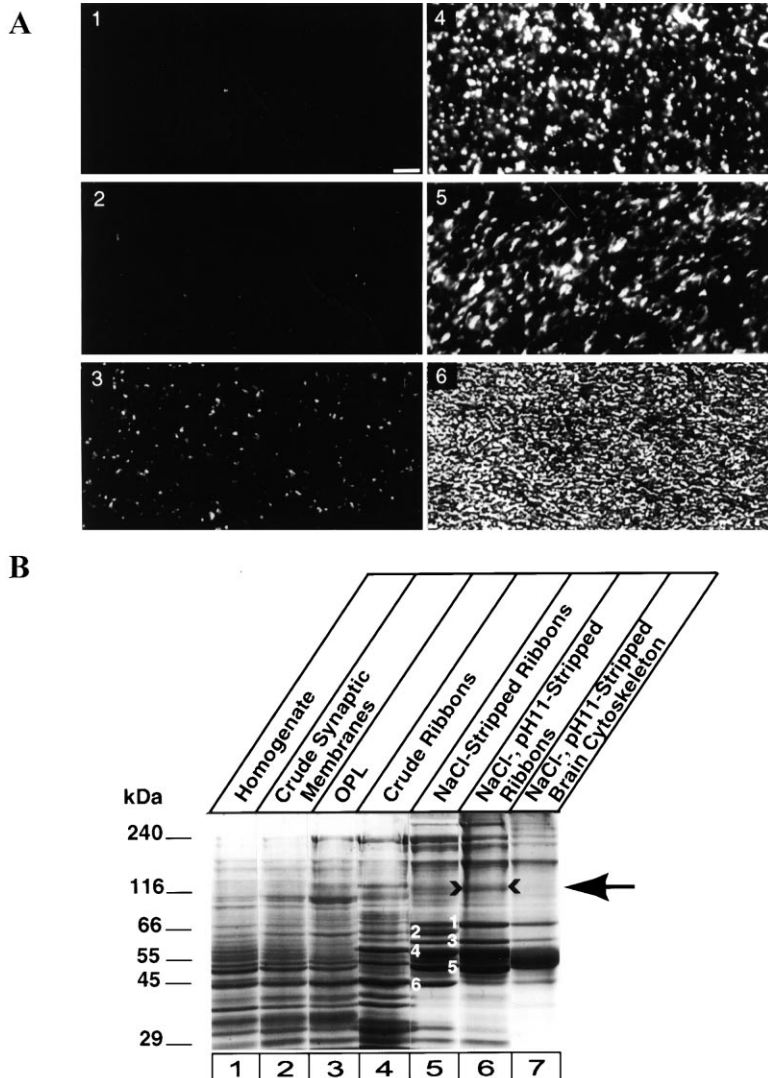§To whom correspondence should be addressed (e-mail: tsudho@mednet.swmed.edu).

A

B

Figure 1. Purification of Synaptic Ribbons from Bovine Retina Analyzed by Immunofluorescence Microscopy or SDS–PAGE and Coomassie Blue Staining

(A) Immunofluorescence analysis. Fractions obtained during the purification of synaptic ribbons were pelleted sectioned on a cryostat, and stained with a ribbon-specific antibody (Schmitz et al., 1996). Fractions analyzed were (1) crude homogenate, (2) crude synaptic membranes, (3) OPL fraction, (4) crude synaptic ribbons, (5) NaCl-stripped synaptic ribbons, and (6) NaCl-, pH 11-stripped synaptic ribbons. Scale bar, 3 μm. (B) The same fractions analyzed in (A) by immunofluorescence were subjected to SDS–PAGE and Coomassie blue staining. In addition, a cytoskeletal protein fraction from brain was analyzed in lane 7; this fraction was isolated from brain by the same procedure as the highly purified ribbons from retina in lane 6 in order to detect cytoskeletal contaminants from true ribbon proteins in lane 6. In lane 5, the proteins labeled by white numbers were identified by sequencing as follows: (1) low-molecular weight neurofilament subunit, (2) novel protein unrelated to any databank sequence, (3) vimentin, (4) GFAP, (5) tubulin, and (6) actin. The 220 kDa doublet was identified as spectrin by immunoblotting (not shown). A 120 kDa protein (marked by an arrow) is the major protein that is selectively enriched in the ribbon fraction but not the brain cytoskeletal fraction and was named RIBEYE. Numbers on the left indicate positions of molecular weight markers.

they generally contain the same proteins as conventional synapses (Ullrich and Südhof, 1994; Brandstätter et al., 1996a, 1996b; von Kriegstein et al., 1999). Only minor differences were observed, such as the use of syntaxin 3 instead of syntaxin 1 for fusion (Morgans et al., 1996) and of L-type Ca^{2+} channels instead of N-, P/Q-, or R-type channels for Ca^{2+} influx (Heidelberger and Matthews, 1992; Nachman-Clewner et al., 1999). Furthermore, rabphilin and synapsins are absent from ribbon synapses in some but not all species (Mandell et al., 1990; von Kriegstein et al., 1999). However, the absence of rabphilin is unlikely to be functionally important, since a knockout of *rabphilin* has no measurable phenotype in conventional synapses (Schlüter et al., 1999), and the significance of the absence of synapsins is similarly uncertain since expression of synapsin I in photoreceptor synapses does not alter synaptic transmission (Geppert et al., 1994).

In contrast to the detailed knowledge about the morphology, physiology, and overall protein complement of the terminals of ribbon synapses, little is known about the composition of the ribbons themselves. Morphologically, synaptic ribbons have the appearance of a cy-

toskeletal structure with a lamellar organization (Sterling, 1998). However, no cytoskeletal protein has been localized to ribbons, nor do they have the typical filaments that are characteristic of various types of cytoskeleton. Only one protein has been localized to ribbons, the presynaptic active zone protein RIM, which interacts with the vesicle protein rab3 as a function of GTP (Wang et al., 1997). In addition, the kinesin motor protein KIF3A is associated with ribbons as well as other organelles in the presynaptic nerve terminal (Muresan et al., 1999). The localization of RIM to ribbons appears to be rather specific since other active zone proteins such as bassoon and munc13-1 (Brandstätter et al., 1999; F.S. and N. Brose, unpublished data) do not localize to ribbons but only to the active zone. Together, these results suggest that ribbons are not composed of known components but are assembled from a novel class of proteins specific for the ribbons. Understanding the structure of ribbons will be necessary for insight into the mechanism by which these fascinating synapses prime vesicles for rapid continuous release. In addition, such understanding may provide clues to deciphering genetic diseases, since ribbon components would be

Figure 2. Primary Structures of Rat, Human, and Bovine RIBEYE: Relation to CtBPs and D Isomer–Specific 2-Hydroxyacid Dehydrogenases

(A) Domain structures of RIBEYE, CtBP2, CtBP1, and phosphoglycerate dehydrogenase. RIBEYE is composed of a unique N-terminal A domain and a C-terminal B domain that is identical with CtBP2 and homologous to phosphoglycerate dehydrogenases. The percentage sequence identity between the various protein domains is shown between the bar diagrams.

(B) Amino acid sequences of human, rat, and bovine RIBEYE (identified on the left as hRE, rRE, and bRE, respectively) are aligned with the sequences of human CtBP1 and CtBP2 (hC1 and hC2, respectively; accession numbers P56545 and Q13363), *Methanococcus jannaschii* phosphoglycerate dehydrogenase (mPD; accession numbers U67544 and L77117), and a consensus sequence of D isomer–specific 2-hydroxyacid dehydrogenases (called DHcs on the left; from Goldberg et al., 1994). Residues in the RIBEYE sequences that are shared among at least two of the three species are highlighted in blue for the RIBEYE unique N-terminal domain (the A domain) and in red for the C-terminal domain that RIBEYE shares with CtBPs (the B domain). Since the C-terminal half of RIBEYE is identical with the entire sequence of CtBP2 except for the N-terminal 20 residues, only a single sequence labeled "hR/C2" is shown in the region corresponding to the RIBEYE B domain. In addition to the CtBP sequences, the C-terminal RIBEYE B domain is also aligned with an archibacterial phosphoglycerate dehydrogenase sequence, because RIBEYE is most homologous to this member of the D isomer–specific 2-hydroxyacid dehydrogenase gene family. A consensus sequence for enzymes of this gene family labeled DHcs is displayed below the RIBEYE, CtBP, and phosphoglycerate dehydrogenase sequences to highlight the conservation of the consensus sequence in RIBEYE and CtBPs. The residues that bind NAD^+ in D isomer–specific 2-hydroxyacid dehydrogenases are highlighted with black background. The arginine (R), glutamate (E), and histidine (H) residues that are essential for catalysis in D isomer–specific 2-hydroxyacid dehydrogenases are identified by a yellow background. Peptide sequences obtained from purified synaptic ribbons from bovine retina are shown in italic green typeface. Sequences are numbered on the right.
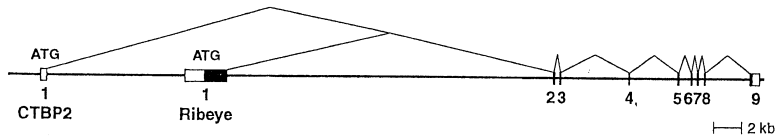
Figure 3. Structure of the Human Gene Encoding RIBEYE and CtBP2

CtBP2 and RIBEYE are transcribed from independent promoters in the same gene in which the unique N-terminal sequences of each protein are included in a single 5′ exon (exon 1), while their shared C-terminal sequences are encoded by eight common 3′ exons (exons 2–9). The genomic organization of RIBEYE/CtBP2 was deduced from the sequence of clone RP11–114N8 (accession number AC013533). Exon 1 of CtBP2 encodes only its N-terminal 20 residues (underlined in 2B), whereas exon 1 of RIBEYE includes the sequence of the entire A domain of RIBEYE.

prime candidates for disorders that selectively affect vision and hearing, for example in various forms of Usher's syndrome. In the current study, we have used large-scale purification of synaptic ribbons from retina as an approach to identify ribbon-specific components. We report the characterization of a component of these ribbons, a protein which we refer to as RIBEYE, whose unexpected structure suggests a pathway of ribbon evolution and whose properties give rise to a model for ribbon function.

Results

Purification of Synaptic Ribbons

In order to gain insight into the components that make up synaptic ribbons, we biochemically purified a fraction enriched in synaptic ribbons from bovine retina. Purification of synaptic ribbons is made difficult by their low abundance, elongated flat shape, and heterogeneity; as a result, little is known about their major components. We hypothesized that as electron-dense structures, synaptic ribbons may resemble pre- and postsynaptic densities and also be detergent insoluble and resistant to extraction with alkaline high-salt solutions. Therefore, we first isolated a crude ribbon fraction from bovine retina by sucrose-gradient centrifugation (Schmitz et al., 1996) and then extracted the ribbons in detergents with buffers containing 2 M NaCl and 0.1 M Na-bicarbonate at pH 11.0. These relatively harsh treatments were intended to remove nonspecifically bound peripheral proteins. The enrichment of ribbons in the fractions and the composition of the fractions were monitored by immunofluorescence microscopy with a ribbon-specific antibody (Figure 1A) and by SDS–PAGE followed by Coomassie blue staining (Figure 1B).

Immunofluorescence staining of the various subcellular fractions was performed with a ribbon-specific anti-body discovered serendipitously as an autoantibody (Schmitz et al., 1996) (Figure 1A). This antibody specifically reacts only with ribbons on tissue sections but does not recognize a protein on immunoblots, possibly because it reacts with a complex epitope or a nonprotein component of synaptic ribbons. Staining of the various fractions revealed that synaptic ribbons are enriched in the crude ribbon fraction and that their purity is further increased upon extraction with alkaline high-salt buffer (Figure 1A). Alkaline extraction appears to break the ribbons into fragments without solubilizing them, as evidenced by the smaller average size of the immunofluorescently labeled particles and as confirmed by electron microscopy (data not shown). The purification of ribbons by this procedure is consistent with the notion that synaptic ribbons are not membranous but are composed of a stable protein aggregate.

Analysis of the purified synaptic ribbons by SDS–PAGE uncovered an coenrichment of a defined set of polypeptides with the ribbons (Figure 1B). However, the ribbon purification procedure resembles methods for isolating cytoskeletal proteins, especially intermediate filaments that are insoluble in detergents or at alkaline pH. Since in retina the cytoskeleton is far more abundant than ribbons, this raises the concern that some or all of the proteins purified in the ribbon fraction may in fact be derived from cytoskeletal impurities and not from actual ribbons. To identify proteins that are truly specific for synaptic ribbons, we isolated a cytoskeletal fraction from brain (which contains virtually no ribbons) by exactly the same procedure as that used for purification of ribbons from retina. Direct comparison of the most pure, identically prepared fractions from retina and brain revealed that the majority of the proteins in the retina and brain fractions are identical, supporting the suspicion that most of the proteins in the most pure ribbon fraction are not specific for ribbons (lanes 6 and 7, Figure
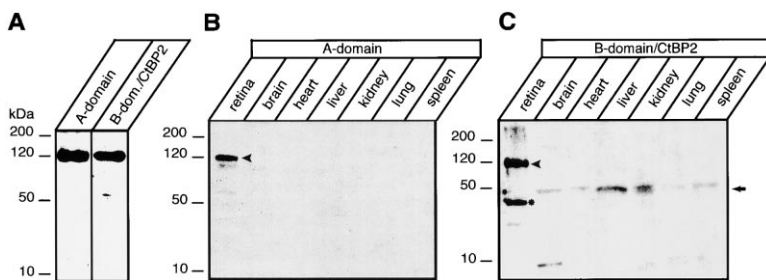

Figure 4. Immunoblotting Analysis of Bovine Tissues with A and B Domain–Specific Antibodies

(A) Comparison of RIBEYE immunoreactivity in purified ribbon fractions (see Figure 1) with A and B domain–specific antibodies.

(B and C) Analysis of proteins from the indicated tissues with A and B domain–specific antibodies, respectively. Note that the A domain antibody only recognizes RIBEYE in retina (arrowhead), whereas the B domain antibody detects an additional low-abundance 50 kDa protein in all tissues; this protein presumably corresponds to CtBP2 (arrow). The lower band observed with the B domain antibody in (C) (asterisk) but not in (A) is smaller than CtBP2 and probably represents a proteolytic breakdown product, since the B domain of RIBEYE is very sensitive to proteolysis. Numbers on the left indicate positions of molecular weight markers. All signals were developed with enhanced chemiluminescence.
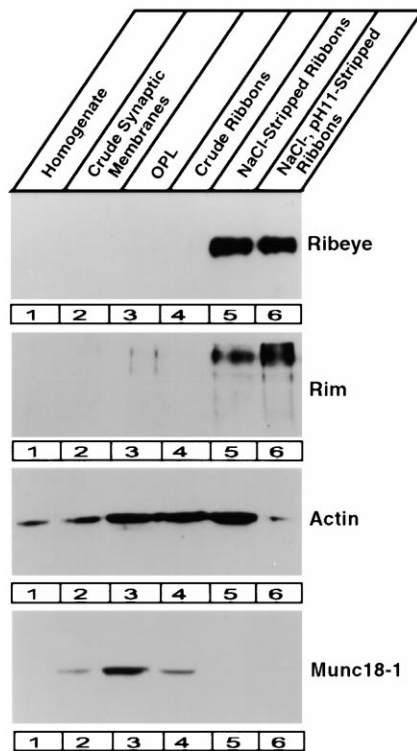
Figure 5. Enrichment of RIBEYE with RIM but Not with Other Synaptic Markers during Purification of Synaptic Ribbons

The fractions obtained during ribbon isolation described in Figure 1 were subjected to immunoblotting analysis using the A domain–specific antibody with enhanced chemiluminescence detection. Since equivalent amounts of sample were loaded on all lanes, the overall low abundance of RIBEYE and RIM in retina allows detection of these proteins only at the level of sensitivity applied in the purified fractions (lanes 5 and 6). In contrast, the more abundant actin and munc18-1 are found in less pure fractions but are deenriched in the purified ribbon samples.

1A). This was confirmed by direct peptide sequencing of some of the proteins, which identified GFAP, vimentin, neurofilaments, internexin, tubulin, and actin (Figure 1B). We observed only two proteins that were enriched in the ribbon fraction from retina but absent from the similarly isolated brain fraction, suggesting that these two proteins are major components of synaptic ribbons. The first protein is a novel protein of ~120 kDa (arrow in Figure 1B) that we named RIBEYE in reference to the synaptic *rib*bon as the subcellular organelle in which it resides and the *eye* as the tissue of origin. The second protein of ~63 kDa was not identified based on partial peptide sequences (data not shown) and was not studied further.

Structure of RIBEYE

To clone RIBEYE, we obtained partial peptide sequences from the protein purified with synaptic ribbons (Figure 1B) and used the sequences to isolate cDNA clones by standard methods (see Experimental Procedures). In this manner, we determined the full-length primary sequences of rat, human, and bovine RIBEYE. These sequences predict a protein of 984–988 residues

that is highly conserved in vertebrates (Figure 2). The cDNA sequences were judged to be "full length" based on three criteria: (1) recombinant RIBEYE expressed by transfection in HEK293 cells had the same electrophoretic mobility as endogenous RIBEYE from bovine retina (data not shown), (2) the sequences of the human and bovine cDNAs contained multiple stop codons 5′ to the proposed translation start site, and (3) the putative initiator codons in the cDNAs were preceded by Kozak consensus sequences.

Analysis of the human, rat, and bovine amino acid sequences of RIBEYE revealed that RIBEYE is composed of two parts, an N-terminal A domain (565 residues) and a C-terminal B domain (420 residues) (Figure 2). Databank searches showed that the A domain is not significantly homologous to any currently described protein and is rather unremarkable except for a relative abundance of serine and proline residues. Surprisingly, however, the B domain was found to be identical to CtBP2, a nuclear protein that together with CtBP1 constitutes a family of transcription repressors (Schaeper et al., 1995; Katsanis and Fisher, 1998; Poortinga et al., 1998; Turner and Crossley, 1998; Zhang and Levine, 1999). CtBP1 was originally identified as a C-terminal binding protein for the adenovirus E1A-protein, and CtBP2 was subsequently observed as a close structural and functional homolog of CtBP1 (see references cited above).

The RIBEYE B domain contains the full-length CtBP2 sequence except the 20 N-terminal amino acids of CtBP2. The sequence identity between the B domain and CtBP2 suggests that these proteins are transcribed from the same gene. This hypothesis was confirmed in databank analyses, which identified a single contiguous human genome sequence that includes the complete gene for CtBP2 and RIBEYE (clone RP11-114N8; GenBank accession number AC013533). In the genomic sequence, the unique N-terminal sequences of CtBP2 and RIBEYE are each encoded by separate 5′ exons, whereas their shared C-terminal sequences are contained within eight common 3′ exons (Figure 3). The first exon of CtBP2 is 5′ to the first exon of RIBEYE, which is therefore located in the middle of the large first intron of the CtBP2 gene. Since CtBP2 only has 20 residues of unique sequence that are not present in RIBEYE, its first exon is relatively small. In contrast, the first RIBEYE exon is large, since it codes for 565 residues. The fact that the A and B domains of RIBEYE and CtBP2 are encoded by the same gene, in addition to the independent cloning of the RIBEYE mRNA from three different vertebrate species, provides evidence that the presence of CtBP2 in the RIBEYE sequence is not a cloning artifact. Interestingly, searches of the *Drosophila* and *C. elegans* genome sequences demonstrated that although they each contain a CtBP homolog, no sequences with significant similarity to the A domain of RIBEYE could be detected (data not shown). The 5′ intron in the vertebrate CtBP2 gene that contains the first exon of RIBEYE (Figure 3) is absent from the *Drosophila* genome sequence. Thus, the generation of a protein similar to RIBEYE by alternative promoters and 5′ exons in the CtBP gene is not possible in *Drosophila*, supporting the notion that RIBEYE and retinal synaptic ribbons are an evolutionary innovation of vertebrates.
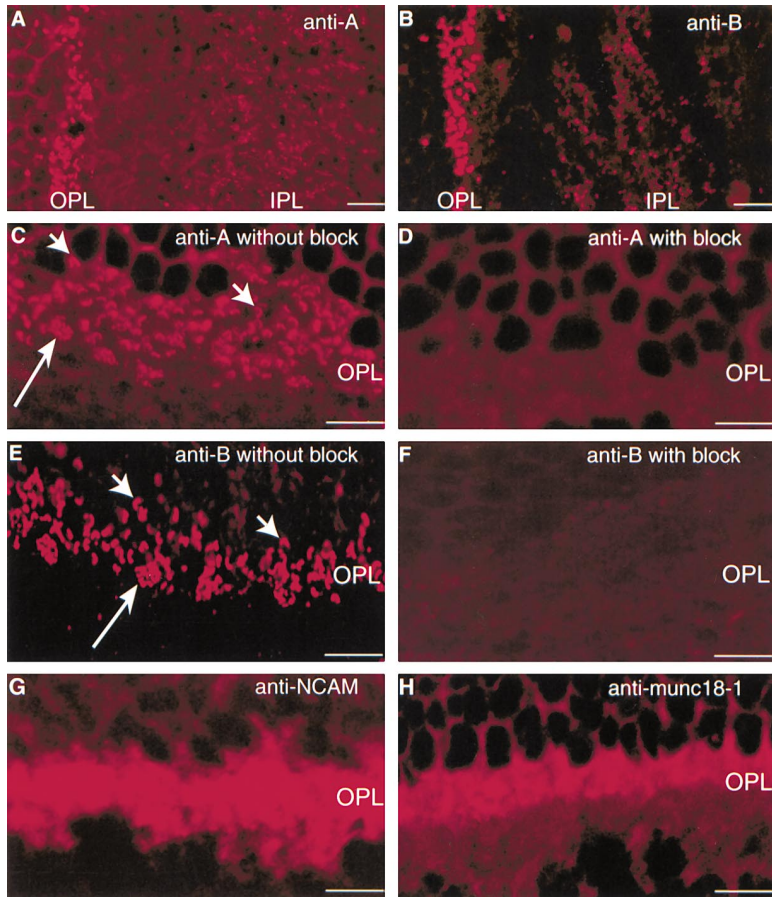
Figure 6. Imunofluorescence Localization of RIBEYE in Bovine Retina Using Antibodies to the A and B Domains

(A and B) Cross-sections of bovine retina immunolabeled with antibodies to the A and B domains of RIBEYE (referred to as anti-A and anti-B, respectively). Locations of the IPL and the OPL are indicated. Note the strong staining of the OPL, whereas immunopositive puncta in the IPL corresponding to ribbon synapses are sparse. Scale bar, 10 μm.

(C–F) Higher magnification views of the OPL immunolabeled with the anti-A and anti-B antibodies without (C and E) and with (D and F) blockage of the antibody with an excess of the recombinant protein used to raise the antibodies. Horseshoe-shaped structures that are typical for ribbons are organized as single entities close to the outer nuclear layer of the OPL (short arrows) and into groups closer to the inner nuclear layer (long arrows).

(G and H) Similar high magnification views of the OPL immunolabeled for NCAM (G) and munc18-1 (H). Note the uniform labeling of the OPL in a wide band for NCAM (G) and a narrower band for munc18-1 (H) corresponding to the overall synaptic terminals.

All pictures are confocal images. Scale bar, 8 μm (C–H).

The structure of RIBEYE and its gene thus suggest that RIBEYE is a hybrid protein in which a preexisting protein (CtBP2) was joined to a novel N-terminal domain in order to create a fusion protein with a new function. This view is supported by RNA blotting and by immunoblotting experiments with probes specific for the A and B domains of RIBEYE. mRNAs containing the A domain were detected only in the retina, whereas mRNAs containing the B domain (which corresponds to CtBP2) were observed ubiquitously in most tissues, although at variable levels (data not shown). To confirm this at the protein level, we raised independent antibodies to the A and B domains of RIBEYE. Immunoblotting analysis showed that both antibodies recognized RIBEYE specifically as a single 120 kDa band in bovine retina but not in other tissues (Figure 4). No other protein besides RIBEYE was detected with the A domain antibody, while the B domain/CtBP2 antibody reacted in all tissues with a low-abundance protein of ~50 kDa that most likely corresponds to CtBP2. These data support the notion that RIBEYE is transcribed from the common RIBEYE/CtBP2 gene in only a restricted subset of tissues, whereas CtBP2 is widely expressed in all tissues.

RIBEYE Is Specific for Synaptic Ribbons

To ensure that RIBEYE is a specific component of synaptic ribbons, we employed the RIBEYE antibodies to determine its localization. First, we analyzed the fraction obtained during purification of ribbons by immunoblotting (Figure 5). At the sensitivity level of the immunoblot shown, RIBEYE was highly coenriched with RIM in the purified ribbons, whereas actin and munc18-1 were deenriched. We then performed immunofluorescence staining of cryostat sections from bovine retina, showing that both RIBEYE antibodies intensely reacted with synapses present at high density in the outer plexiform layer (OPL) and low density in the inner plexiform layer (IPL) (Figure 6). The OPL is a narrow synaptic zone of the retina at which rod and cone photoreceptor cells generate ribbon synapses with horizontal and bipolar cells (Sterling, 1998). The IPL is a broader synaptic zone composed of ribbon synapses from bipolar cells and classical synapses elaborated by amacrine cells (reviewed by Dowling, 1987). In both synaptic zones, RIBEYE immunoreactivity exhibited a discrete punctate pattern. The horseshoe-like appearance of the structures labeled by RIBEYE in the OPL and their localization as isolated or clustered puncta are typical for synaptic ribbons in rod and cone photoreceptor synapses, respectively (short and long arrows in Figures 6C and 6E, respectively; see Schmitz et al., 1996, Wang et al., 1997). This pattern is quite different from the immunolabeling obtained with antibodies that react with the entire synaptic zone, such as antibodies to NCAM or munc18-1 (Figure 6). The antibodies to the A and B domains gave similar staining patterns (e.g., compare Figures 6A and 6B or 6C and 6E). These results confirm that RIBEYE is only present in small structures within the synaptic zone but does
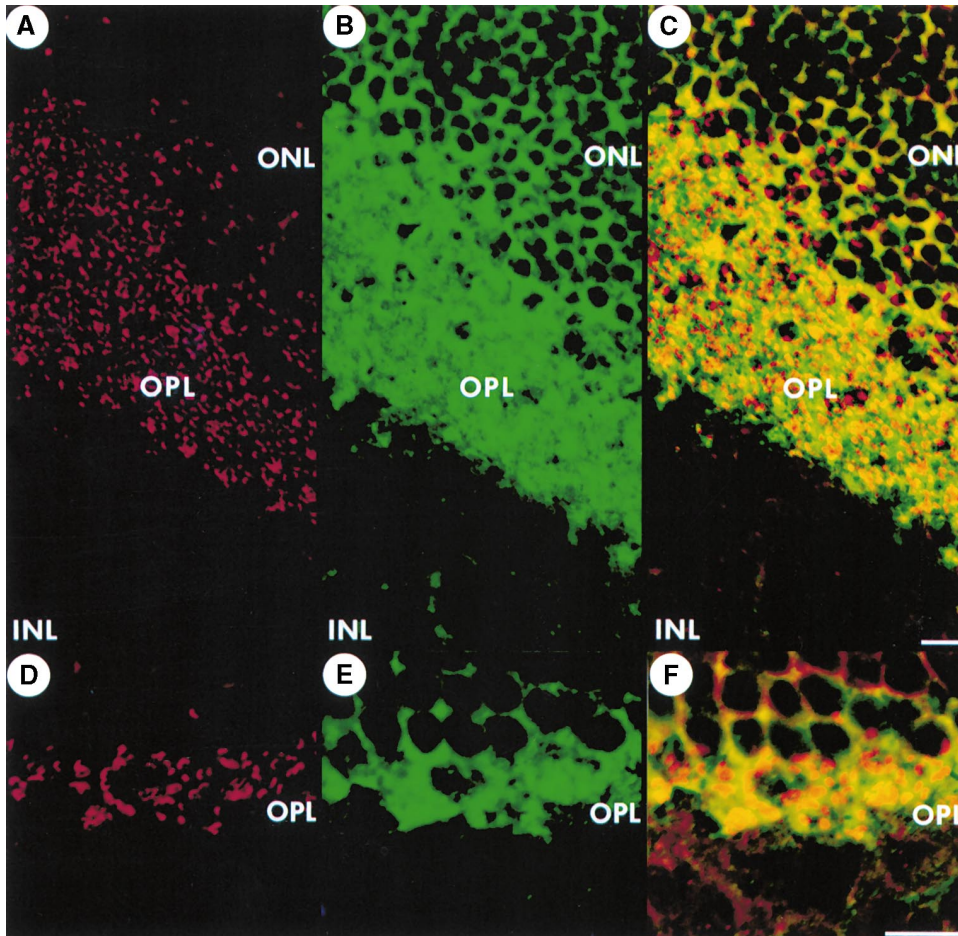
Figure 7. Double Labeling of Bovine Retina by Immunofluorescence for RIBEYE and the Synaptic Vesicle Protein Synaptophysin

Cryostat sections of the bovine retina were cut in two different planes and double-immunolabeled with polyclonal antibodies to the B domain of RIBEYE (A and D) and a monoclonal antibody to synaptophysin (B and E). In (C) and (F), images are merged to display overlapping structures, which are shown in yellow, demonstrating that all the RIBEYE-positive puncta are located within the overall nerve terminals stained by synaptophysin. Scale bar, 7 μm.

not actually fully occupy the entire presynaptic terminal. No nuclear staining was observed with the B domain antibodies that recognize CtBP2, probably because the levels of CtBP2 in the nucleus are much lower than those of RIBEYE in synaptic ribbons, of which it is a major component. The reactivity of the A and the B domain antibodies could be blocked by addition of excess antigen used to raise the antibody, suggesting that their staining was specific (Figure 6).

To relate the staining pattern for RIBEYE to the localization of nerve terminals, we performed double immunofluorescence labeling experiments of the OPL with antibodies to RIBEYE and to synaptophysin, a synaptic vesicle protein that serves as a marker for nerve terminals (Navone et al., 1986) (Figure 7). In contrast to the punctate appearance of RIBEYE immunoreactivity, synaptophysin was present throughout the entire synaptic zone. This agrees well with the fact that most of the OPL is occupied by presynaptic nerve terminals, which in turn are filled with synaptic vesicles (Geppert et al., 1994). Superposition of the RIBEYE- and synaptophysin-labeled structures revealed that all RIBEYE puncta

are located within the synaptophysin-positive nerve terminals (Figure 7). Again, both antibodies to RIBEYE resulted in similar staining patterns, while preimmune sera gave no specific staining (data not shown).

To confirm that RIBEYE is specifically and exclusively localized to synaptic ribbons, we used immunogold electron microscopy on ultrathin resin-embedded sections of bovine retina (Figure 8). Both RIBEYE antibodies exclusively labeled synaptic ribbons. The very high density of immunogold particles decorating the ribbons suggests that, as expected from the exclusive enrichment of RIBEYE with synaptic ribbons during the biochemical purification (Figure 1B), RIBEYE must be abundant in the synaptic ribbons even though it is not an abundant protein in retina homogenate (Figure 8). The immunolabeling was specific, since antibodies to control proteins (e.g., synaptotagmin, munc18-1, NCAM, and tubulin) produced a different staining pattern that did not associate with the ribbons (Figure 8 and data not shown). No significant labeling by the RIBEYE antibody was observed outside of synaptic ribbons.

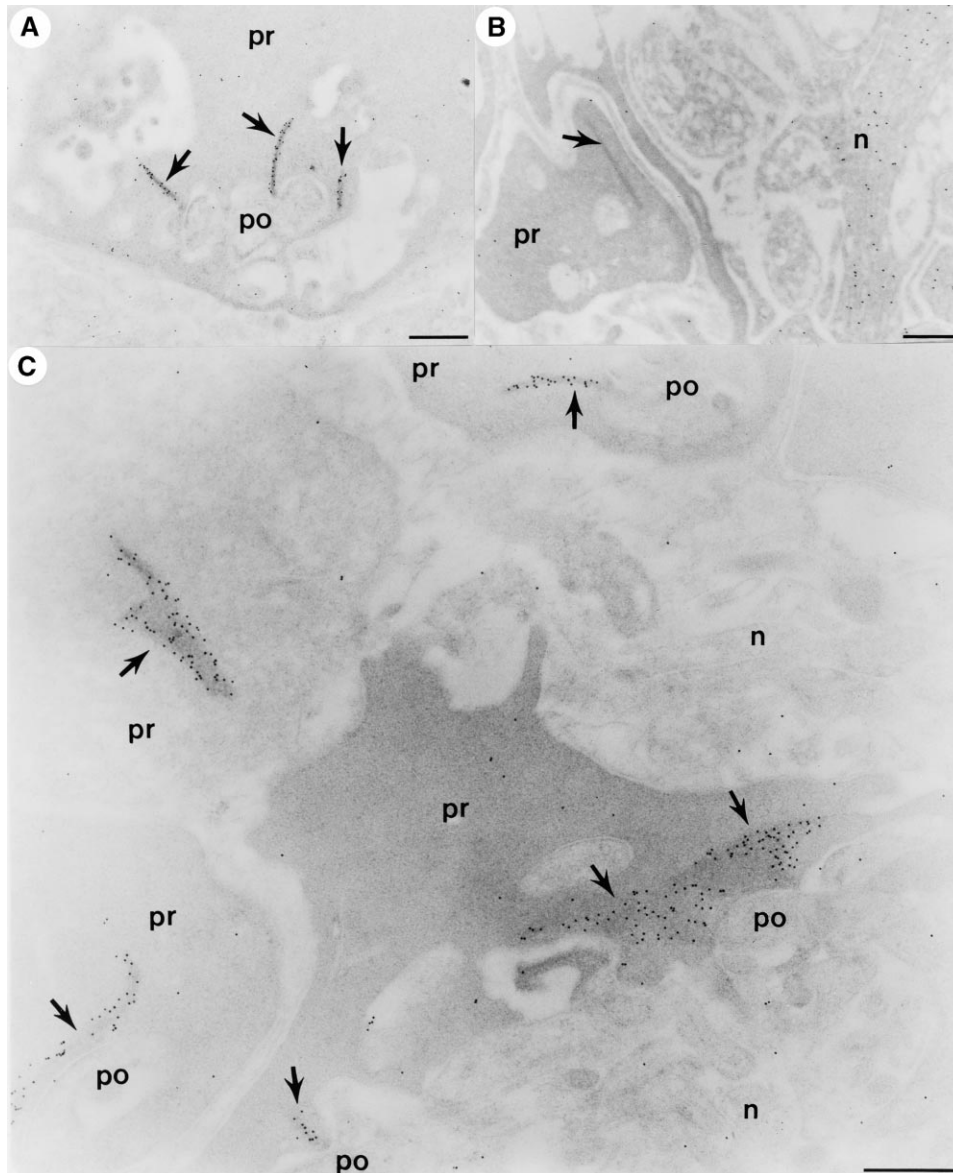The immunocytochemistry results demonstrate that

Figure 8. Immunogold Localization of RIBEYE in Synaptic Ribbons by Electron Microscopy

Ultrathin sections of bovine retina were immunolabeled with two different antibodies to RIBEYE (A and C) and to tubulin (B). Immunopositive areas were visualized with 10 nm gold–conjugated secondary antibodies. Both RIBEYE antibodies specifically stained synaptic ribbons (arrows), whereas the tubulin antibody strongly labeled neurites ("n" in [B]) but not synaptic ribbons. Abbreviations: po, postsynaptic process; pt, presynaptic terminal. Scale bars, 250 nm (A and B); 200 nm (C).

RIBEYE is a specific component of synaptic ribbons in the OPL and IPL of the retina. No RIBEYE immunoreactivity was detected on immunoblots in brain, nor was RIBEYE mRNA observed by RNA blotting (Figure 4 and data not shown), indicating that RIBEYE is not a general component of all synapses. However, presynaptic structures similar to ribbons are observed in the pineal gland and in cochlear hair cells in addition to the retina (Smith and Sjöstrand, 1961; Hopsu and Arstila, 1964; Jastrow et al., 1997; Lenzi et al., 1999). To test if RIBEYE may be a component of similar presynaptic bodies outside of the retina, we performed immunocytochemistry experiments on brain sections (Figure 9). No significant reactivity in cortex was observed, whereas the pineal gland was strongly labeled. Labeling was specific, as it

could be blocked with the antigen. This result indicates that RIBEYE may be a general component of synaptic ribbons.

Domain-Specific Aggregation of RIBEYE in Transfected Fibroblasts

Our results characterize ribbons as stable structures that can only be dissolved in denaturing solutions such as SDS and probably contain a limited number of protein components (Figure 1). The nature of RIBEYE as a fusion protein in which a specific N-terminal domain is coupled to a C-terminal transcriptional repressor suggests that the former conveys a ribbon-specific function to the latter. One possibility is that the A domain may function in the assembly of ribbons as insoluble protein aggre-
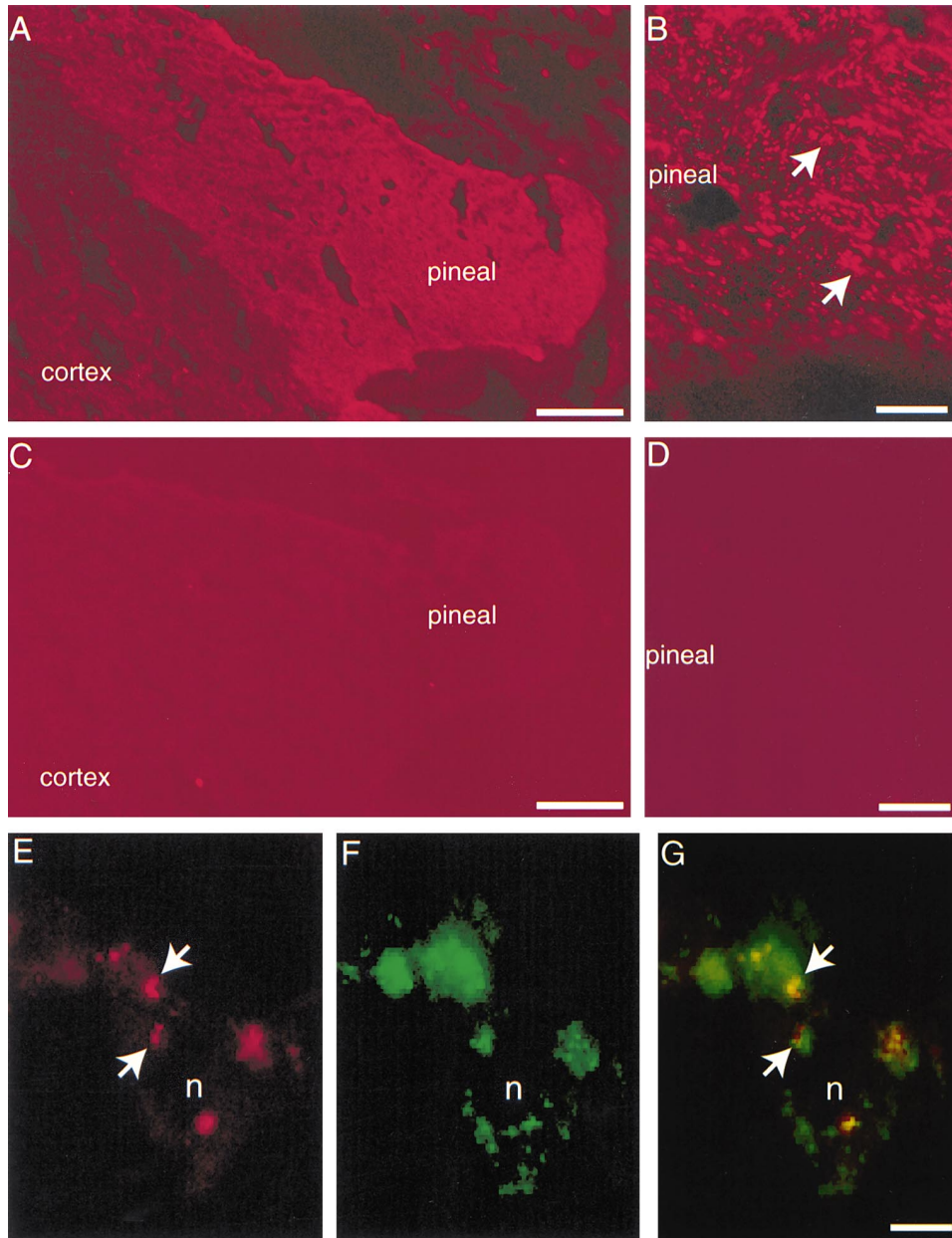
Figure 9. Immunofluorescence Localization of RIBEYE in Rat Pineal Gland

Cryostat sections from rat brain were stained with antibodies to the B domain of RIBEYE (A and B) or preimmune serum (C and D) or double-labeled with polyclonal antibodies to RIBEYE and monoclonal antibodies to synaptobrevin 2 (E and F). The relative locations of the pineal gland and the cortex are indicated in (A) through (D). Arrows identify ribbons; "n" in (E) through (G) marks the location of the nucleus. Scale bars, 250 μm (A and C); 8 μm (B and D); and 3 μm (E–G).

gates. To test this hypothesis, we expressed full-length RIBEYE and its A and B domains by transfection in HEK293 fibroblasts. Expression of full-length RIBEYE, either fused to a myc epitope tag or to enhanced green fluorescent protein (EGFP), resulted in the formation of large immunoreactive structure in HEK293 cells (Figures 10A and 10B). The same formation of large immunoreactive particles was observed upon transfection of the A domain fused to EGFP (Figure 10C). In contrast, expressed B domain fused to EGFP was diffusely present throughout the cytoplasm and entirely soluble (Figure 10D and data not shown), as was EGFP alone (Figure

10E). This result suggests that the A domain has an intrinsic ability to form aggregates, indicating that the A domain may function in the formation of stable ribbon structures, whereas the B domain may be exposed on the surface of the ribbons.

RIBEYE/CtBP2 Is a NAD$^+$ Binding Protein Related to 2-Hydroxyacid Dehydrogenases

The design of RIBEYE as a fusion protein of a novel domain with a preexisting transcription factor suggests an intriguing evolutionary history, an accidental origin of RIBEYE in the vertebrate lineage by serependipitous
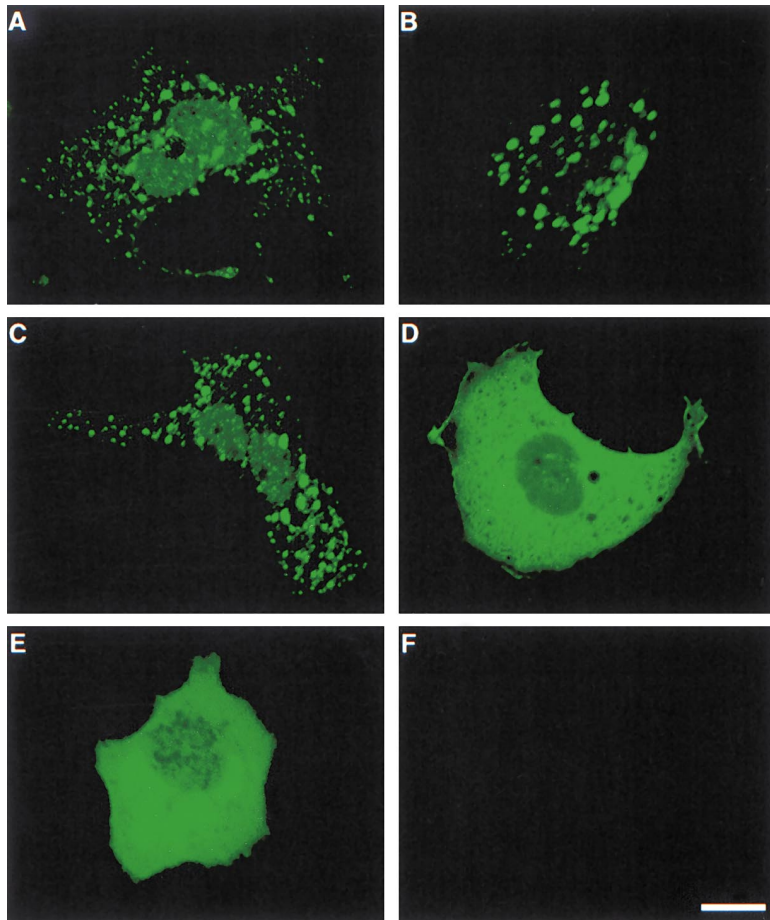
Figure 10. The A Domain of RIBEYE Triggers Aggregate Formation in Transfected 293 Cells

HEK293 cells were transfected with DNA vectors encoding the following proteins: full-length RIBEYE containing a myc epitope tag at the N terminus (A and F); full-length RIBEYE fused to EGFP at the C terminus (B), the A or B domain of RIBEYE separately fused to EGFP (C and D, respectively), and EGFP alone without RIBEYE (E). RIBEYE was visualized in (A) by immunocytochemistry using an anti–myc epitope monoclonal antibody and Cy2-conjugated secondary antibody, and in (B) through (E) by direct fluorescence of EGFP. (F) represents a control processed as in (A) but without the primary anti–myc epitope antibody. The scale bar in (F) equals 4 μm and applies to all panels.

addition of an exon excoding the A domain to the preexisting CtBP2 gene. However, further analyses indicate that the evolutionary history of RIBEYE may be even more complex and give a clue to the possible function of the B domain. As noted previously (Schaeper et al., 1995; Turner and Crossley, 1998), CtBP1 and CtBP2 themselves are not novel in terms of sequence but are significantly homologous to enzymes of the family of NAD^+-dependent 2-hydroxyacid dehydrogenases. This homology is illustrated in Figure 2B in the alignment of the sequences of RIBEYE and CtBPs with that of phosphoglycerate dehydrogenase from the archibacterium *Methanococcus jannaschii*, the 2-hydroxyacid dehydrogenase protein to which RIBEYE and CtBPs are most homologous. In addition, Figure 2B presents an alignment of all of these sequences with a consensus sequence for NAD^+-dependent 2-hydroxyacid dehydrogenases (from Goldberg et al., 1994). Interestingly, most of the residues in the dehydrogenase consensus sequence are conserved in CtBPs and RIBEYE, including in particular the four residues that are involved in binding NAD^+ (GXGXXG-18-D; black in Figure 2B) and the three amino acids that function in catalysis (R-30-E-19-H; yellow in Figure 2B). This conservation suggests that RIBEYE and CtBPs may still be partly or completely enzymatically active.

To test this idea, we analyzed NAD^+ binding to a recombinant glutathione S-transferase (GST) fusion protein of the B domain of RIBEYE/CtBP2, with GST as a negative control (Figure 11). Strong and specific binding of ^{14}C-labeled NAD^+ was observed. Scatchard analysis uncovered a single class of binding sites in RIBEYE/CtBP2 with an affinity of ~1.3 μM NAD^+. ^{14}C-NAD^+ binding was completely inhibited by a 100-fold excess of unlabeled NAD^+ or by Cibacron blue, which serves as a common ligand for NAD^+ binding sites in many proteins (Thompson and Stellwagen, 1976), but was unaffected by serine (Figure 11). These results suggest that the homology of the RIBEYE B domain/CtBP2 to NAD^+-dependent 2-hydroxyacid dehydrogenases is functionally important, and that the domain may serve as an enzyme in synaptic vesicle priming on synaptic ribbons and in transcriptional repression.

Discussion

Ribbon synapses are unusual synapses dedicated to fast tonic neurotransmitter release. They are only found in a subset of specialized neurons: photoreceptor cells and bipolar cells in the retina, cochlear hair cells in the ear, and melatonin-secreting neurons of the epiphysis (Smith and Sjöstrand, 1961; Hopsu and Arstila, 1964; Dowling, 1987; Sterling, 1998; Borjigin et al., 1999; Lenzi et al., 1999). Apart from the epiphysis, where the function of the ribbons is unclear, ribbon synapses have thus evolved as essential components of the two sensory
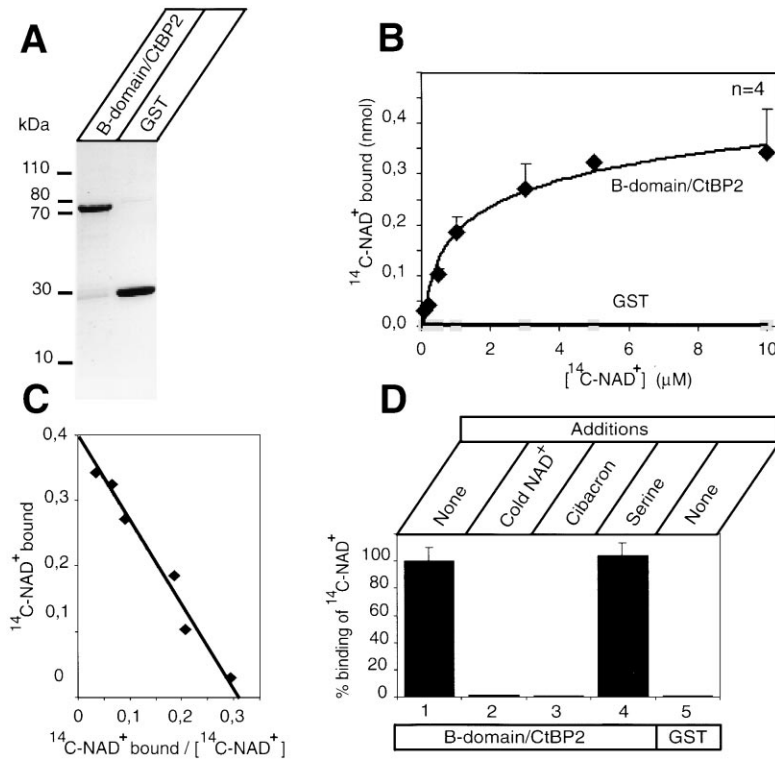
Figure 11. Binding of NAD$^+$ to the B Domain of RIBEYE/CtBP2

(A) SDS–PAGE analysis of proteins used for binding measurements, the GST fusion protein of the B domain of RIBEYE (left lane), and GST alone (right lane). The picture shows a Coomassie blue–stained gel with positions of molecular weight standards on the left.

(B) Binding of ^{14}C-labeled NAD$^+$ to the GST-RIBEYE fusion protein or GST alone (n = 4; error bars indicate SEM).

(C) Scatchard analysis of the binding data shown in (B). The calculated K_d = 1.3 μM NAD$^+$.

(D) Specificity of NAD$^+$ binding to the B domain of RIBEYE. Binding of 10 μM ^{14}C-labeled NAD$^+$ in the absence of competitor (column 1, 100%) is displaced completely by 1 mM cold NAD$^+$ (column 2) or 1 mM cibacron blue 3GA, an NAD$^+$ analog (column 3) but not by 1 mM serine (column 4). Column 5 shows binding to GST alone as background binding.

systems that are most characteristic of vertebrates: hearing and vision. With their special physiological properties, ribbon synapses provide vision and hearing with a degree of signal discrimination that is unparalleled in other senses. This is achieved by graded tonic release of neurotransmitters, which allows transfer of a continuous stream of information (Dowling, 1987; Juusola et al., 1996). At chemical synapses, neurotransmitters are released by synaptic vesicle exocytosis under utilization of similar proteins for all synapses and organisms studied (reviewed by Fernandez-Chacon and Südhof, 1999). The high rate of tonic release from ribbon synapses demands much faster vesicle traffic than can be achieved at a normal synapse. However, immunocytochemical studies have shown that the components of ribbon synapses are generally similar to those of conventional synapses (Ullrich and Südhof, 1994; Brandstätter et al., 1996a, 1996b; von Kriegstein et al., 1999). Although there are some differences between the two types of synapses (e.g., see Morgans et al., 1996; Nachman-Clewner et al., 1999), their vesicles appear to be built from the same proteins, and the same mechanisms seem to be used for fusion and Ca^{2+} triggering. Therefore the same fundamental apparatus for mediating neurotransmitter release is probably used in ribbon and in conventional chemical synapses, with the ribbons constituting the major difference. It is likely that the primary function of the ribbons is to speed up vesicle traffic by serving as a conduit for synaptic vesicles. As a first step toward an understanding of how ribbons perform this function, we have now partially purified synaptic ribbons and studied one of their most abundant protein components, which we named RIBEYE.

Our data demonstrate that ribbons are composed of a stable protein aggregate that contains RIBEYE as a major constituent. RIBEYE is built from two domains, an A domain that is not homologous to any known protein but forms spontaneous protein aggregates upon heterologous expression in 293 cells, and a B domain that is identical to a well-studied transcription factor, CtBP2. The fusion of a transcription factor to a novel sequence in a synaptic protein is unexpected and raises important concerns about the validity of this observation. Five lines of evidence demonstrate, however, that the fusion of the unique ribbon-specific A domain with a known transcription factor as the B domain is not a cloning artifact but created an evolutionarily novel component of synaptic ribbons. First, the same structure for RIBEYE was independently deduced from multiple overlapping cDNA clones isolated from three different species (Figure 2). Second, the genomic sequences of RIBEYE and CtBP2 showed that they are encoded by a single gene but are transcribed from distinct promoters and include different first exons containing the unique sequences of RIBEYE and CtBP2 (Figure 3). Third, RIBEYE protein was identically detected with antibodies to both domains at the size predicted from the cDNA sequences (Figure 4 and data not shown). Fourth, antibodies to both domains of RIBEYE localized the protein to synaptic ribbons (Figures 5 and 6). Fifth and finally, RIBEYE is not detectable in the *Drosophila* and *C. elegans* genome sequences available in GenBank, whereas CtBP is present in these genomes. The *Drosophila* genome contains only a single CtBP gene that lacks an N-terminal intron at the position at which the human gene contains the first intron preceded by alternative first exons and promoters for CtBP2 and RIBEYE.

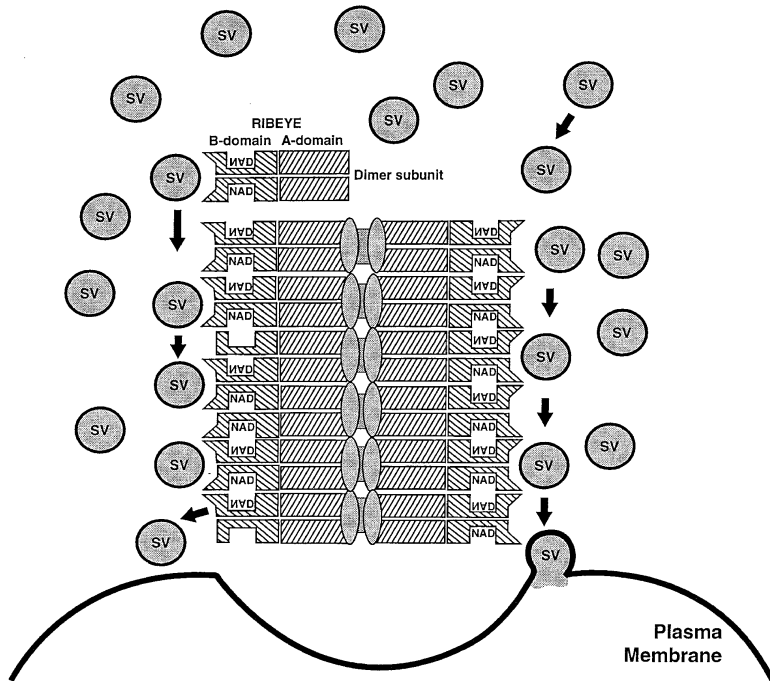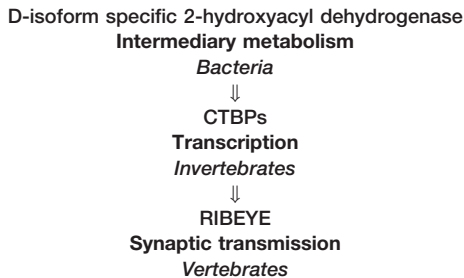The structure of RIBEYE suggests a mechanism for

Figure 12. Working Model for the Role of RIBEYE in the Function of Synaptic Ribbons

RIBEYE is displayed in the ribbons as a protein aggregate formed by its A domain, with the NAD binding B domain (which is identical to CtBP2) exposed on the surface to interact with an unknown component of synaptic vesicles (SV), analogous to the function of CtBP2 in the nucleus as a binding partner for transcription factors. The B domain is depicted as a dimer since CtBP2 is a dimer (Poortinga et al., 1998). The model suggests that RIBEYE is a major component of ribbons in addition to other proteins, some of which are schematically indicated as inner-core protein. This protein may correspond to the second unique protein besides RIBEYE that was found in the biochemically purified ribbon fraction (Figure 1).

the evolutionary emergence of ribbon synapses in vertebrates. It demonstrates that RIBEYE was built by fusing a novel sequence encoded in a single exon to an existing protein with a completely different function. This indicates that the evolution of RIBEYE and ribbons required the recruitment of a novel exon into the genomic sequences encoding the N terminus of CtBP2. As a result, the following evolutionary scheme is proposed:

D-isoform specific 2-hydroxyacyl dehydrogenase
Intermediary metabolism
Bacteria
⇓
CTBPs
Transcription
Invertebrates
⇓
RIBEYE
Synaptic transmission
Vertebrates

It almost appears as though synaptic ribbons could have been created by a beneficial evolutionary accident when a large exon was connected with CtBP2. The use of a transcriptional repressor as a fusion partner for a presynaptic ribbon protein is ingenious, since at the synapse no transcription occurs; thus, the transcription factor cannot cause unwarranted effects locally at the synapse by performing its normal function on top of its new synaptic function. It is possible that in the case of the DNA replication factor latheo, another example of a protein that normally functions in the nucleus also shown to be important for synapses (Rohrbough et al., 1999), a similar logic applies.

A possible model for the function of RIBEYE is shown in Figure 12. This model, to be considered only as a working hypothesis to guide future investigations, hypothesizes that the N-terminal A domain is involved in

the formation of the assembled proteinaceous ribbon as a protein aggregate as suggested by the behavior of the A domain transfected into 293 cells. According to this model, RIBEYE alone is not sufficient to organize ribbons but requires at least one additional protein component indicated in the model as an inner-core protein. The presence of such a protein component is suggested by the finding of a second unique protein in the biochemically purified ribbon fraction, which we have not yet identified (Figure 1). A function for the B domain, which is identical with CtBP2, is indicated by the normal role of CtBP2 in the nucleus as a transcriptional suppressor and by the high-affinity binding of NAD^+ observed here. As a transcriptional repressor, CtBP2 functions by binding to other transcription factors via a consensus sequence (PXDLS), although it is unclear precisely how it acts to depress transcription (Schaeper et al., 1995; Nibu et al., 1998; Turner and Crossley, 1998). Our observation that the domain binds NAD^+ with high affinity (Figure 11) indicates that its homology with NAD^+-dependent dehydrogenases is functionally relevant and that it may in fact serve as an enzyme. It is interesting the CtBP1, a close homolog of CtBP2, was recently also suggested to function in membrane traffic under the name of "BARS" (brefeldin A-ADP ribosylated substrate) (Weigert et al., 1999). BARS was discovered because it, together with glyceraldehyde phosphate dehydrogenase (GAPDH), is the major ADP-ribosylated substrate in tissue culture cells (Di Girolamo et al., 1995). It was proposed that CtBP1, as BARS, has a role in membrane fission in the Golgi complex by functioning as a lysophosphatidic acid coenzyme A acyltransferase (Weigert et al., 1999). The close structural relationship of CtBPs with NAD^+-dependent dehydrogenases agrees well with the finding that CtBP is ADP ribosylated in an NAD^+-dependent reaction in parallel with GAPDH (another NAD^+-dependent dehydrogenase) (Di Girolamo et al.,

1995). However, this relationship also makes it difficult to imagine how CtBP1 could function as a coenzyme A–dependent acyltransferase, since there is little chemical similarity between the reaction mechanisms of acyl-transferases and dehydrogenases, raising questions about the precise enzymatic role of CtBP1 in Golgi membrane traffic.

Overwhelming evidence shows that CtBPs are transcriptional repressors in a large number of organisms, indicating that their NAD$^+$ binding and possible enzymatic function may be involved in executing this function. As mentioned above, CtBPs function in transcription not by binding DNA directly but by interacting with specific DNA binding proteins (Schaeper et al., 1995; Nibu et al., 1998; Turner and Crossley, 1998). The binding sequences for CtBPs in their target proteins share a consensus sequence characterized by a PXDLS motif. By analogy, we would like to suggest as a working hypothesis that the B domain of RIBEYE (which is identical with CtBP2) is displayed on the surface of the ribbons (Figure 12). On the ribbon surface, RIBEYE then is proposed to interact with a target sequence containing the consensus motif PXDLS of CtBPs. This model suggests that the target sequence may be in a synaptic vesicle protein and that this interaction may be involved in docking and/or translocation of vesicles. Furthermore, it is conceivable that an unknown enzymatic reaction of the B domain may be involved in priming. Although highly speculative at present, this model would provide a parsimonious explanation for how ribbons evolved and how they work. Identification of the binding partners for the B domain on the ribbon surface and the role of NAD$^+$ binding in their function will give valuable insight into how this domain might perform this proposed function.

Experimental Procedures

Purification of Synaptic Ribbons from Bovine Retina and Analysis of Protein Components by Amino Acid Sequencing

Synaptic ribbons were partially purified from bovine retina essentially as described (Schmitz et al., 1996). Briefly, bovine retinae were homogenized for 3 min on ice with an Ultraturrax Type TP 18/10 (Janke and Kunkel, Staufen Germany) in buffer A (15 mM Na$_2$HPO$_4$ [pH 7.4], 1 mM EGTA, 1 mM MgCl$_2$, and 1 mM PMSF). The crude homogenate was layered on a 50% sucrose cushion in buffer A and centrifuged for 50 min at 15,000 rpm at 4°C in a JA20 rotor (Beckman, Palo Alto, CA). After dilution with a 2-fold volume of buffer A and subsequent spin at 20,000 rpm in a JA20 rotor, the washed membranes were loaded onto a linear sucrose gradient (35%–50% w/v in buffer A) and centrifuged in an SW40 rotor at 13,000 rpm for 75 min. The OPL fraction was recovered at 40% sucrose and lysed with 1% Triton X-100 at a protein concentration of ~1 mg/ml for 30 min on ice. The Triton lysate was layered onto a sucrose step gradient (2 ml of 30%, 40%, 50%, and 70% sucrose [w/v] in buffer A) and centrifuged at 11,000 rpm for 75 min at 4°C. The synaptic ribbon fraction was recovered at the interface between 50% and 70% sucrose and further purified by extraction with 2 M NaCl in PBS or 2 M NaCl in 0.1 M Na$_2$CO$_3$ (pH 11.0) for 15 min at 4°C followed by centrifugation (15 min in an Eppendorf tabletop centrifuge at 14,000 rpm). A fraction from bovine brain neocortex was prepared similarly. Proteins present in the various fractions were analyzed by SDS–PAGE, immunoblotting, and sequencing essentially as described (Johnston et al., 1989). For amino acid sequencing, bands were recovered after SDS–PAGE from nitrocellulose blots, digested with trypsin, and subjected to Edman degradation in an Applied Biosystems automatic peptide gas-phase sequencer.

Molecular Cloning of RIBEYE and Sequence Analyses

Bovine retinae were isolated within 20 min after death and flash-frozen in liquid nitrogen. Poly-A enriched mRNA was purified from the frozen retinas, using a Qiagen mRNA purification kit according to the manufacturer's specification, and quantified by UV absorption at 260 nm and 280 nm. Purified mRNA (0.4 μg) was used for first-strand cDNA synthesis using "superscript" reverse transcriptase and second-strand cDNA synthesis as described by Hoffman and Gubler (1983) using RNase H, *E. coli* DNA polymerase I, and *E. coli* DNA ligase (all from Gibco BRL). Double-stranded cDNA was used for PCR with two sets of primers. Degenerate oligonucleotides derived from a RIBEYE peptide sequence (YGAEAPAYPTGQVYNNAK; primer 1, CGCAAGCTTACGG[CTAG]GC[CTAG]GA[AG]GC; primer 2, GCGAAGCTT[CTAG]GC[AG]TT[AG]TT[AG]TA; nucleotides in brackets indicate redundant positions), with a 69 bp product. Primer 1 was combined in PCR reactions with primer 3 derived from another peptide sequence (GALLPGDYYSDPAGAAR, primer 3, CCAGGG GA[CT]TA[CT]AG[CT]GA [CT]CC), resulting in a 309 bp product. PCR products were subcloned into pBluescript, confirmed by sequencing, and employed to screen rat and bovine retina cDNA libraries in λZAPII (Stratagene) and a human retina cDNA library in λgt10 essentially as described (Sambrook et al., 1989). Clones isolated in the initial screens were then used in subsequent screens to isolate cDNAs covering the entire coding regions of rat, bovine, and human RIBEYE (Figure 2). The 5' end of the bovine cDNA was obtained with a 5' RACE strategy using the marathon cDNA kit of Clontech and a forward anchor primer 4 (CCATCCTAATACGACTCACTA TAGGGC) and a gene-specific, reverse primer deduced from the cloned 309 bp PCR product (primer 5, GGGTCGCTGTAATAG TCCCCTGG). All DNAs were sequenced using ABI automatic DNA sequencers. All DNA sequences were analyzed with DNA star software; databank searches were performed using the NCBI program suite with public DNA and protein sequence databanks.

Construction of RIBEYE Expression Vectors
prRE-EGFP Encoding Full-Length Rat RIBEYE Fused to EGFP in pEGFP-N1

The stop codon of the rat RIBEYE cDNA was replaced with an additional BamHI site by PCR to allow in-frame cloning of rat RIBEYE into pEGFP-N1 (Clontech). First the C-terminal region of rat RIBEYE from the EcoRI site at ~2.8 kb to the new BamHI site was cloned into the correponding sites of pEGFP-N1 (resulting vector denoted as pCtermrRE-EGFP). Then, the ~2.8 kb 5' EcoRI fragment of the full-length rat RIBEYE clone containing the start ATG were subcloned into pCtermrRE-EGFP, using analytical BamHI digests to verify the orientation of the 2.8 kb fragment.

prRE-9E10myc Encoding Full-Length Rat RIBEYE Fused to the Myc Epitope in p9E10myc3

The ~1.3 kb EcoRI-BglII and the ~2.6 kb BglII-XhoI fragments of rat RIBEYE were cloned into the EcoRI and SalI sites of pCMV9E10myc3, resulting in a vector containing full-length rat RIBEYE with an N-terminal myc tag.

pA-rRE-EGFP Encoding the A Domain of Rat RIBEYE in pEGFP

The A domain of rat RIBEYE was PCR amplified with primers 6 (CTAGAATTCTTTGCTCTGCCAATGCCGGTT) and 7 (AGTGGATC CATACTTGGTTCTGGTGTTAGCATGG), and the product was cloned into the EcoRI and BamHI sites of pEGFP-N1 (Clontech).

pA-RE-9E10myc Encoding the A Domain of Rat RIBEYE in p9E10myc

The 0.7 kb EcoRI-EcoRV insert fragment from rat RIBEYE and the 1.0 kb EcoRV-BamHI fragment of pA-rRE-EGFP were cloned into the EcoRI and BamHI sites of pCMV9E10myc3.

pB-rRE-EGFP Encoding the B Domain of Rat RIBEYE in pEGFP-N1

A ~1 kb EcoRI fragment from an in vivo–excised λZAP cDNA clone of RIBEYE containing the B domain plus seven additional residues preceeded by a Kozak consensus sequence was cloned into the EcoRI site of pCtermrRE-EGFP. The orientation of the cloned EcoRI fragment was analyzed by restriction with NotI.

pA-bRE-GexKG

The cDNA of the bovine RIBEYE sequence coding for residues 107–209 was amplified by PCR, and the product was cloned into the EcoRI and XhoI sites of pGEX-KG.

pB-rRE-GexKG

The complete B domain of the rat (Figure 2) was amplified by PCR, using primers that included SpeI and XhoI sites used for cloning into the XbaI and XhoI sites of pGEX-KG.

Protein Expression in HEK293 Cells

HEK293 cells cultured in DMEM with 10% FBS were transfected using the DEAE-dextran transfection method as described (Ichtchenko et al., 1995). Cells were incubated with the DNA-DEAE dextran complexes for 30 min at 37°C, treated with chloroquine (100 mM) for 3 hr at 37°C, and exposed to medium containing 20% glycerol for 2 min at room temperature. Protein expression was analyzed 48–72 hr after transfection.

Antibodies

Antibodies against the bovine A domain (antibody name: Winden) and rat B domain of RIBEYE (name: U2656) were generated in rabbits as described (Johnston et al., 1989), using the purified GST fusion proteins encoded by pA-bRE-GexKG and pB-rRE-GexKG. Both antisera were used for immunofluorescence microscopy in a 1:500 dilution, for postembedding immunoelectron microscopy in a 1:2000 dilution, and for immunoblotting in a 1:5000 dilution. All other antibodies were described previously: autoantibody against synaptic ribbons (Schmitz et al., 1996; used for immunofluorescence microscopy in a 1:500 dilution); polyclonal antisera against RIM (Q703 and R809; Wang et al., 1997; used for Western blotting in a 1:1000 dilution); monoclonal antibody against synaptophysin (clone 43.1, gift of Dr. R. Jahn; used for immunofluorescence microscopy in a 1:200 dilution); monoclonal antibody against actin (AC40, Sigma; used for Western blotting in a 1:5000 dilution); polyclonal antibody against munc18-1 (TCS; used for Western blotting in a 1:5000 dilution); monoclonal antibody to NCAM (Sigma, anti-HNK-1/NCAM [CD57], clone VC1.1; Naegele and Barnstable, 1991; used for Western blotting in a 1:1000 dilution); monoclonal antibody against β-tubulin (Tub 2.1, Sigma; used for immunogold electron microscopy in a 1:2000 dilution); and monoclonal antibody against myc tag (Santa Cruz; used for immunofluorescence microscopy at a 1:200 dilution).

Immunocytochemical Analysis of the Localization of RIBEYE

Immunofluorescence microscopy on retinal sections and fractions of the bovine retina was performed largely as previously described (Schmitz et al., 1996; Schmitz and Drenckhahn, 1997; von Kriegstein et al., 1999). Freshly isolated, chemically unfixed tissues/retinal fractions were flash-frozen in liquid nitrogen–cooled isopentane (tissues) or directly in liquid nitrogen (retinal fractions). From these samples, 10 μm cryostat sections were cut with a FrigoCut2800 (Reichert-Jung). For immunofluorescence detection of proteins expressed in transfected 293 cells, cells were briefly washed with PBS and fixed with 1% formaldehyde in PBS for 30 min at room temperature. Cells and cryostat sections were treated with blocking buffer (0.5% BSA in PBS containing 0.2% Triton-X100) for 45 min at room temperature, and primary antibodies diluted in blocking buffer were added for overnight incubations at 4°C. Thereafter, cells and sections were washed multiple times with blocking buffer, secondary antibodies were added (Cy2/Cy3-conjugated goat-anti-rabbit antibodies for polyclonal rabbit primary antibodies, or Cy2/Cy3-conjugated goat-anti-mouse antibodies for monoclonal mouse primary antibodies [all from Jackson Labs], at 1:800 dilutions in blocking buffer) and incubated for 1 hr at room temperature. After subsequent washes with blocking buffer (four times, each for 5 min) and then PBS (four times, each for 5 min), cells were mounted in 60% glycerol in PBS that contained 1.5% n-propyl gallate in order to retard photobleaching. Samples were analyzed and documented with a confocal laser scanning microscope (MRC1024, BioRad). Controls were performed by omitting primary antibodies and by using only secondary antibody or by using irrelevant primary antibodies (antibodies to actin, tubulin, NCAM, and munc18-1; see above). For assembling figures, confocal images were transformed from the BioRad "pic" to "tiff" formats.

Immunogold Electron Microscopy

Immunogold electron microscopy was performed largely as previously described (Schmitz and Drenckhahn, 1993). Bovine retina fixed with 2% freshly depolymerized paraformaldehyde, 0.1% glutaraldehyde in PBS for 3 hr at 4°C were washed with PBS (six times, each for 10 min) and infiltrated with 0.5% tannic acid (Mallinckrodt) in PBS (1 hr at 4°C). After extensive washes with H_2O, retinae were treated with 2% uranylacetate for 3 hr in 4°C, dehydrated with ascending concentrations of ethanol, and embedded in LR-Gold resin (London resins) using benzil (0.5%) as a catalyst. Ultrathin sections (70 nm) were cut and collected on uncoated 100 mesh gold grids. Sections were preincubated with 0.5% BSA in PBS, grids were transferred to primary antibody dilutions (antibodies to the A and B domains of RIBEYE at a 1:2000 dilution in 0.5% BSA in PBS), and primary antibodies were detected by goat anti-rabbit secondary antibodies conjugated to 10 nm gold particles (Sigma). After extensive washing with PBS, immunogold complexes were fixed with 2.5% glutaraldehyde in PBS, and sections were contrasted with 2% uranyl acetate for 20 min at room temperature and analyzed either with a Zeiss EM 902 or with a Jeol JEM2010 electron microscope. Controls were performed by either omitting the primary antibody or using irrelevant mono- and polyclonal antibodies, e.g., monoclonal and polyclonal antibodies against tubulin and the respective secondary antibodies.

RNA Blotting Analysis

For Northern blotting analysis of retinal RNA, ~4 μg of purified retinal mRNA was treated with formamide and formaldehyde prior to electrophoresis on denaturing formaldehyde agarose gels (Sambrook et al., 1989) with RNA length standards II from Boehringer/Mannheim. mRNAs were blotted onto Hybond N+ membrane (Amersham) in 20× SSC overnight at room temperature and then UV-crosslinked to the membranes. Northern blots for all other tissues were obained on multitissue blots from Clontech. Blots were hybridized, washed, and exposed as described (Sambrook et al., 1989; Ichtchenko et al., 1995).

Miscellaneous Procedures

SDS–PAGE and immunoblotting analyses were performed using standard procedures as described previously (Johnston et al., 1989; Ichtchenko et al., 1995). After electrophoretic transfer of proteins to nitrocellulose, unspecific protein binding sites were blocked by preincubating the membranes in PBS containing 5% skim milk powder and 0.2% Tween 20 for 45 min at room temperature. Primary antibodies diluted in blocking buffer were added at the concentrations indicated above. Incubations with primary antibodies was performed overnight at 4°C. Binding of the primary antibodies was detected with secondary antibodies conjugated to HRP (Jackson Laboratories, diluted 1:5000 in blocking buffer for 1 hr at room temperature) by enhanced chemiluminescence detection (Amersham). Protein concentrations were determined by a Coomassie blue–based protein assay kit (BioRad).

References

Borjigin, J., Li, X., and Snyder, S.H. (1999). The pineal gland and melatonin: molecular and pharmacologic regulation. Annu. Rev. Pharmacol. Toxicol. *39*, 53–65.

Brandstätter, J., Wässle, H., Betz, H., and Morgans, C.W. (1996a). The plasma membrane protein SNAP-25, but not syntaxin, is present at photoreceptor and bipolar cell synapses in the rat retina. Eur. J. Neurosci. *8*, 823–828.

Brandstätter, J.H., Löhrke, S., Morgans, C.W., and Wässle, H. (1996b). Distributions of two homologous synaptic vesicle proteins,

synaptoporin and synaptophysin, in the mammalian retina. J. Comp. Neurol. 370, 1–10.

Brandstätter, J.H., Fletcher, E.L., Garner, C.C., Gundelfinger, E.D., and Wassle, H. (1999). Differential expression of the presynaptic cytomatrix protein bassoon among ribbon synapses in the mammalian retina. Eur. J. Neurosci. 11, 3683–3693.

Di Girolamo, M., Silletta, M.G., De Matteis, M.A., Braca, A., Colanzi, A., Pawlak, D., Rasenick, M.M., Luini, A., and Corda, D. (1995). Evidence that the 50-kDa substrate of brefeldin A-dependent ADP-ribosylation binds GTP and is modulated by the G-protein beta gamma subunit complex. Proc. Natl. Acad. Sci. USA 92, 7065–7069.

Dowling, J.E. (1987). The Retina: An Approachable Part of the Brain. (Cambridge, MA: Harvard University Press).

Fernandez-Chacon, R., and Südhof, T.C. (1999). Genetics of synaptic vesicle function towards the complete functional anatomy of an organelle. Annu. Rev. Physiol. 61, 753–776.

Geppert, M., Ullrich, B., Green, D.G., Takei, K., Daniels, L., De Camilli, P., Südhof, T.C., and Hammer, R.E. (1994). Synaptic targeting domains of synapsin I revealed by transgenic expression in photoreceptor cells. EMBO J. 13, 3720–3727.

Goldberg, J.D., Yoshida, T., and Brick, P. (1994). Crystal structure of a NAD-dependent D-glycerate dehydrogenase at 2:4 Å resolution. J. Mol. Biol. 236, 1123–1140.

Gray, E.G., and Pease, H.L. (1971). On understanding the organisation of the retinal receptor synapses. Brain Res. 35, 1–15.

Gubler, U., and Hoffman, B.J. (1983). A simple and very efficient method for generating cDNA libraries. Gene 25, 263–269.

Heidelberger, R., and Matthews, G. (1992). Calcium influx and calcium current in single synaptic terminals of goldfish retinal bipolar neurons. J. Physiol. (Lond.) 447, 235–256.

Hopsu, V.K., and Arstila, A.U. (1964). An apparent somato-somatic synaptic structure in the pineal gland of the rat. Exp. Cell Res. 37, 484–487.

Ichtchenko, K., Hata, Y., Nguyen, T., Ullrich, B., Missler, M., Moomaw, C., and Südhof, T.C. (1995). Neuroligin 1: a splice site–specific ligand for b-neurexin. Cell 81, 435–441.

Jastrow, H., von Mach, M.A., and Vollrath, L. (1997). The shape of synaptic ribbons in the rat pineal gland. Cell Tissue Res. 287, 55–261.

Johnston, P.A., Jahn, R., and Südhof, T.C. (1989). Transmembrane topography and evolutionary conservation of synaptophysin. J. Biol. Chem. 264, 1268–1273.

Juusola, M., French, A.S., Uusitalo, R.O., and Weckstrom, M. (1996). Information processing by graded-potential transmission through tonically active synapses. Trends Neurosci. 19, 292–297.

Katsanis, N., and Fisher, E.M. (1998). A novel C-terminal binding protein (CTBP2) is closely related to CTBP1, and adenovirus E1A-binding protein, and maps to human chromosome 21q21.2. Genomics 47, 294–299.

Lenzi, D., Runyeon, J.W., Crum, J., Ellisman, M.H., and Roberts, W.M. (1999). Synaptic vesicle populations in saccular hair cells reconstructed by electron tomography. J. Neurosci. 19, 119–132.

Mandell, J.W., Townes-Anderson, E., Czernik, A.J., Cameron, R., Greengard, P., and De Camilli, P. (1990). Synapsins in the vertebrate retina: absence from ribbon synapses and heterogeneous distribution among conventional synapses. Neuron 5, 19–33.

Morgans, C.W., Brandstätter, J.H., Kellerman, J., Betz, H., and Wässle, H. (1996). A SNARE complex containing syntaxin 3 is present in ribbon synapses of the retina. J. Neurosci. 16, 6713–6721.

Muresan, V., Lyass, A., and Schnapp, B.J. (1999). The kinesin motor KIF3A is a component of the presynaptic ribbon in vertebrate photoreceptors. J. Neurosci. 19, 1027–1037.

Nachman-Clewner, M., St. Jules, R., and Townes-Anderson, E. (1999). L-type calcium channels in the photoreceptor ribbon synapse: localization and role in plasticity. J. Comp. Neurol. 415, 1–16.

Naegele, J.R., and Barnstable, C.J. (1991). A carbohydrate epitope defined by monoclonal antibody VC1.1 is found on NCAM and other cell adhesion molecules. Brain Res. 559, 118–129.

Navone, F., Jahn, R., Di Gioia, G., Stukenbrok, H., Greengard, P.,

and De Camilli, P. (1986). Protein p38: an integral membrane protein specific for small vesicles of neurons and neuroendocrine cells. J. Cell Biol. 103, 2511–2527.

Nibu, Y., Zhang, H., Bajor, E., Barolo, S., Small, S., and Levine, M. (1998). dCtBP mediates transcriptional repression by Knirps, Kruppel and Snail in the Drosophila embryo. EMBO J. 17, 7009–7020.

Parsons, T.D., Lenzi, D., Almers, W., and Roberts, W.M. (1994). Calcium-triggered exocytosis and endocytosis in an isolated presynaptic cell: capacitance measurements in saccular hair cells. Neuron 13, 875–883.

Poortinga, G., Watanbe, M., and Parkhurst, S.M. (1998). Drosophila CtBP: a hairy-interacting protein required for embryonic segmentation and hairy-mediated transcriptional repression. EMBO J. 17, 2067–2078.

Rao-Mirotznik, R., Harkins, A.B., Buchsbaum, G., and Sterling, P. (1995). Mammalian rod terminal: architecture of a binary synapse. Neuron 14, 561–569.

Rieke, F., and Schwartz, E.A. (1996). Asynchronous transmitter release: control of exocytosis and endocytosis at the salamander rod synapse. J. Physiol. (Lond.) 493, 1–8.

Rohrbough, J., Pinto, S., Mihalek, R.M., Tully, T., and Broadie, K. (1999). latheo, a Drosophila gene involved in learning, regulates functional synaptic plasticity. Neuron 23, 55–70.

Sambrook, J., Fritsch, E.F., and Maniatis, T. (1989). Molecular Cloning: A Laboratory Manual, Second Edition (Cold Spring Harbor, NY: Cold Spring Harbor Laboratory Press).

Schaeffer, S.F., Raviola, E., and Heuser, J.E. (1982). Membrane specializations in the outer plexiform layer of the turtle retina. J. Comp. Neurol. 204, 253–267.

Schaeper, U., Boyd, J.M., Sulekha, V., Uhlmann, E., Subramanian, T., and Chinnadurai, G. (1995). Molecular cloning and characterization of a cellular phosphoprotein that interacts with a conserved C-terminal domain of adenovirus E1A involved in negative modulation of oncogenic transformation. Proc. Natl. Acad. Sci. USA 92, 10467–10471.

Schlüter, O.M., Schnell, E., Verhage, M., Tzonopoulos, T., Nicholl, R.A., Janz, R., Malenka, R.C., Geppert, M., and Südhof, T.C. (1999). Rabphilin knock-out mice reveal rat rabphilin is not required for rab3 function in regulating neurotransmitter release. J. Neurosci. 19, 5834–5846.

Schmitz, F., and Drenckhahn, D. (1993). Distribution of actin in cone photoreceptor synapses. Histochemistry 100, 35–40.

Schmitz, F., and Drenckhahn, D. (1997). Localization of dystrophin and β-dystroglycan in bovine photoreceptor processes extending into the postsynaptic dendritic complex. Histochem. Cell Biol. 108, 245–255.

Schmitz, F., Bechmann, M., and Drenckhahn, D. (1996). Purification of synaptic ribbons, structural components of the active zone complex in photoreceptor synapses. J. Neurosci. 16, 7109–7116.

Smith, C.A., and Sjöstrand, F.S. (1961). A synaptic structure in the hair cells of the guinea pig cochlea. J. Ultrastruct. Res. 5, 523–556.

Sterling, P. (1998). The retina. In The Synaptic Organization of the Brain, Fourth Edition, G. Shepherd, ed. (New York: Oxford University Press), pp. 205–253.

Stevens, C.F., and Tsujimoto, T. (1995). Estimates for the pool size of releasable quanta at a single central synapse and for the time required to refill the pool. Proc. Natl. Acad. Sci. USA 92, 846–849.

Thompson, S.T., and Stellwagen, E. (1976). Binding of Cibacron blue F3GA to proteins containing the dinucleotide fold. Proc. Natl. Acad. Sci. USA 73, 361–365.

Trujillo-Cenoz, O. (1972). The structural organization of the compound eye in insects. In Handbook of Sensory Physiology, Volume VII/2, Physiology of Photoreceptor Organs, M.G.F. Fuortes, ed. (New York: Springer Verlag), pp. 5–62.

Turner, J., and Crossley, M. (1998). Cloning and characterization of mCtBP2, a co-repressor that associates with basic Krüppel-like factor and other mammalian transcriptional regulators. EMBO J. 17, 5129–5140.

Ullrich, B., and Südhof, T.C. (1994). Distribution of synaptic markers

in the retina: implications for synaptic vesicle traffic in ribbon synapses. J. Physiol. *88*, 249–257.

von Gersdorff, H., Vardi, E., Matthews, G., and Sterling, P. (1996). Evidence that vesicles on the synaptic ribbon of retinal bipolar neurons can be rapidly released. Neuron *16*, 1221–1227.

von Kriegstein, K., Schmitz, F., Link, E., and Südhof, T.C. (1999). Distribution of synaptic vesicle proteins in the mammalian retina identifies obligatory and facultative components of ribbon synapses. Eur. J. Neurosci. *11*, 1335–1348.

Wan, H.I., DiAntonio, A., Fetter, R.D., Bergstrom, K., Strauss, R., and Goodman, C.S. (2000). Highwire regulates synaptic growth in *Drosophila*. Neuron *26*, 313–329.

Wang, Y., Okamoto, M., Schmitz, F., Hofmann, K., and Südhof, T.C. (1997). Rim is a putative Rab3 effector in regulating synaptic-vesicle fusion. Nature *388*, 593–598.

Weigert, R., Silletta, M.G., Spano, S., Turacchio, G., Cericola, C., Colanzi, A., Senatore, S., Mancini, R., Polishchuk, E.V., Salmona, M., et al. (1999). CtBP/BARS induces fission of Golgi membranes by acylating lysophosphatidic acid. Nature *402*, 429–433.

Zhang, H., and Levine, M. (1999). Groucho and dCtBP mediate separate pathways of transcriptional repression in the *Drosophila* embryo. Proc. Natl. Acad. Sci. USA *96*, 535–540.

GenBank Accession Numbers

The sequences reported in this study are accessible in GenBank under the accession numbers AF222711–AF222713.